Front. Optoelectron. China 2010, 3(2): 109–124
DOI 10.1007/s12200-010-0003-2

REVIEW ARTICLE

Asymmetric resonant cavities and their applications in optics and photonics: a review

Yun-Feng XIAO (✉)[1], Chang-Ling ZOU (✉)[2], Yan LI[1], Chun-Hua DONG[2], Zheng-Fu HAN (✉)[2], Qihuang GONG (✉)[1]

1 State Key Lab for Mesoscopic Physics, School of Physics, Peking University, Beijing 100871, China
2 Key Laboratory of Quantum Information, University of Science and Technology of China, Hefei 230026, China

Abstract Asymmetric resonant cavities (ARCs) with smoothly deformed boundaries are currently under intensive study because they possess distinct properties that conventional symmetric cavities cannot provide. On one hand, it has been demonstrated that ARCs allow for highly directional emission instead of the in-plane isotropic light output in symmetric whispering-gallery cavities, such as microdisks, microspheres, and microtoroids. On the other hand, ARCs behave like open billiard system and thus offer an excellent platform to test classical and quantum chaos. This article reviews the recent progresses and prospects for the experimental realization of ARCs, with applications toward highly directional microlasing, strong-coupling light-matter interaction, and highly sensitive biosensing.

Keywords asymmetric resonant cavity (ARC), directional emission, quality factor, whispering gallery mode, chaos

1 Introduction

Optical resonator (or namely optical cavity) represents a key component or platform in nonlinear optics, light emitting diodes, low-threshold micro-sized lasing, enhanced light-matter interaction (cavity quantum electrodynamics (QED) and biosensors), and miniaturized photonic circuit [1]. Up to the present, three representative optical microcavities have been proposed and investigated [2]. The first one is the conventional Fabre-Perot (FP)-type cavities consisting of two concave dielectric or metal mirrors facing each other at a distance of the order of a few 100 μm. FP-type optical cavities are almost utilized in all branches of modern optics, including lasing feedback, optical parametric oscillators, and some interferometers [3,4]. The second type is the nanoscale optical cavities in photonic crystal when a dot or a line defect is introduced [5–7]. The third one is the dielectric optical microcavities supporting whispering gallery modes [8]. They were named after an acoustic analogue observed by Lord Rayleigh, when he studied the acoustical waves propagating along the smooth stone surface of the St. Paul's Cathedral in London, UK (see in Figs. 1(a) and 1(b)). The similar phenomena can also be observed in the Echo Wall in the Temple of Heaven in Beijing, China (see in Figs. 1(c) and 1(d)). This type of microcavities has rotational symmetric boundary, for instance, microspheres, microdisks, microcylinders, and microtoroids, as shown in Fig. 2(a). Viewed in ray optics, optical whispering gallery modes in the circular dielectric cavities can be easily understood with the concept of total internal reflection. As shown in Fig. 2(b), a ray emits from the point A with an output angle χ ($\sin\chi > 1/n$, where n is the refraction index of the cavity material). Then, it will be continually totally reflected on the cavity boundary due to the rotational symmetry. After finite reflections, the ray returns the point A, and it obtains a propagation phase θ. When $\theta = 2k\pi$ ($k = 1,2,3,...$), the propagating field undergoes constructive interference with itself. This means that only whole numbers of wavelengths of light can "fit" around the edge of the circular dielectric cavity. This selectivity causes discrete modes to exist in the cavity, known as whispering gallery modes.

Two crucial parameters of an optical microcavity are the quality factor (Q) and the mode volume (V). For FP-type cavities, high quality factors can be achieved by utilizing the highest reflectivity and the lowest loss mirrors, as well as the most transparent optical elements for their construction. Nevertheless, the highest quality factor of a FP-type microcavity is still of the order of ten millions

Received November 16, 2009; accepted December 17, 2009

E-mail: yfxiao@pku.edu.cn, senew@email.ustc.edu.cn, zfhan@ustc.edu.cn, qhgong@pku.edu.cn

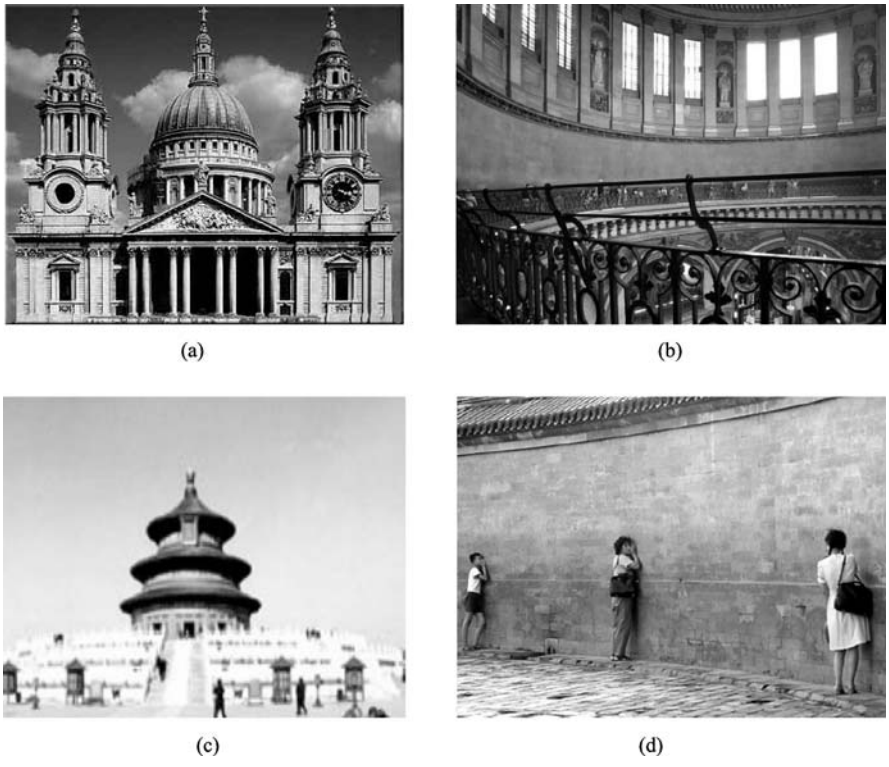

Fig. 1 (a) St. Paul's Cathedral in London; (b) Whispering Gallery in St. Paul's Cathedral in London; (c) Temple of Heaven in Beijing; (d) Echo Wall in Temple of Heaven in Beijing

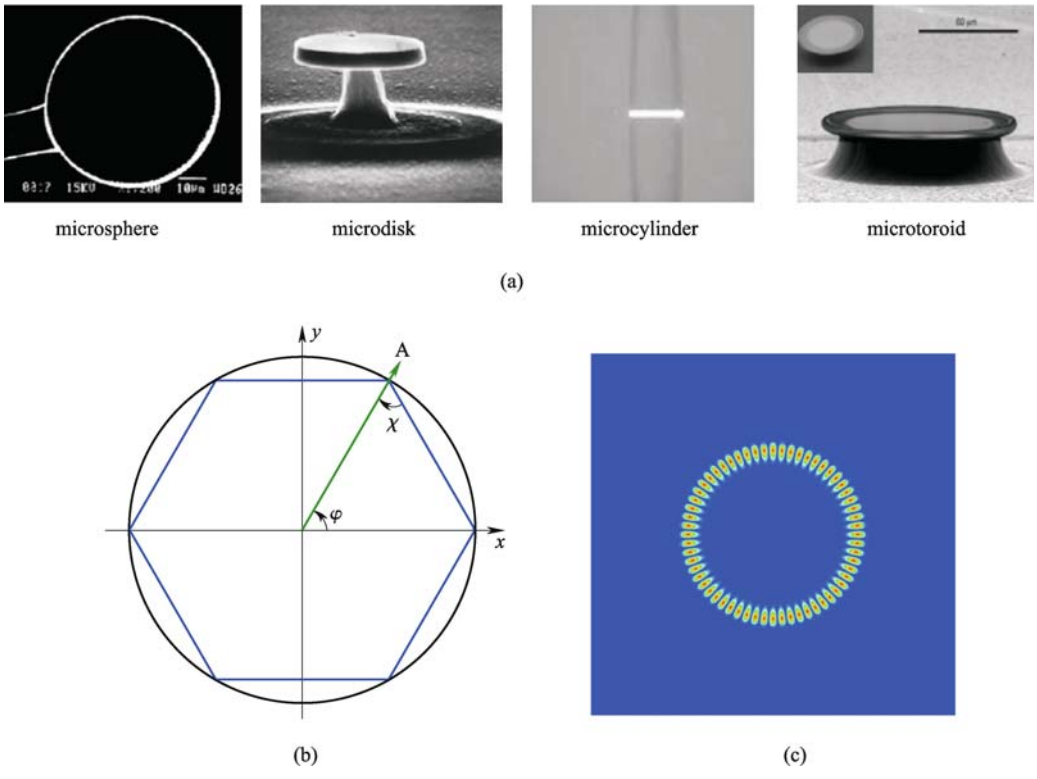

Fig. 2 (a) Four typical whispering gallery microcavities: microspheres [9], microdisks [10], microcylinders [11], and microtoroids [12]; (b) geometrical optics; (c) wave optics representations of a whispering gallery mode

limited by the modern semiconductor technologies [13,14]. For nanocavities in photonic crystal, similarly, the highest quality factor reaches a few millions, which is also restricted by fabrication technologies [15,16]. As a distinguished advantage, whispering gallery microcavities not only have small mode volumes but also possess very high quality factors thanks to the total internal reflection mechanism of the modes. Silica microspheres experimentally exhibit the highest quality factors of nearly 9 billion [17], while the Q factor of a polished crystalline microcavity has been demonstrated to excess 10 billion [18]. The ultrahigh quality factor plays the central role in various applications of microcavities, ranging from narrow-band filter, low-threshold lasing, highly sensitive biomolecule detection, to cavity QED.

Up to the present, in virtue of their high quality factor, small mode volume, and on chip characteristics, optical whispering gallery microcavities have been made huge successes, such as obtaining ultralow threshold lasing on a chip [19,20], realizing strong coupling regime between one neutral atom and a monolithic microresonator [21], and label-free detecting single molecule [22]. However, the emission from whispering gallery modes is isotropic due to the rotational symmetry, which seriously limits their important applications in lots of areas. For instance, microdisk lasers cannot provide controlled directional emission or adequate output power at desired direction though their thresholds are low. Thus, external evanescent-wave elements, such as prisms [23], side-polished fibres [24], and tapped fibres [25] are necessary to efficiently couple light into and out of whispering gallery modes, i.e., constructing the sufficient energy exchange between the coupling elements and the whispering gallery modes. The physical essence of the coupling with the outside is to selectively break the fully rotational symmetry of whispering gallery modes. Besides, the abovementioned phase-matched external couplers, the other natural choice is to design the geometrical shape of microresonators at the very start, leading to a significant modification of the evanescent leakage orientation from whispering gallery modes and appearing as a strongly directional distribution of output fields instead of the isotropic emissions. These resonators are known as asymmetric resonant cavities (ARCs) or deformed cavities, and they are being developed fast over the past few years [26,27].

ARCs not only offer highly directional emission desired for lots of important application but also are used to test classical and quantum chaos because they behave like open billiard systems. In this article, we briefly review the recent progresses and prospects in the area of ARC, with applications in optics and photonics. The rest of this review is organized as follows: In Sect. 2, we shortly introduce the theoretical progress in studying ARCs, including the traditional ray tracing model explanation, the wave solution, the modified ray optical model, and the road to design ARCs possessing both unidirectional emission and high-Q factor. In Sect. 3, we focus our attention on experimental progress in both two- and three-dimensional ARCs. In Sect. 4, we provide some discussion and prospects.

2 Theoretical basis in ARCs

To better understand the experimental results in Sect. 3, we could briefly introduce some basic concept and theoretical method.

2.1 Wave solution of microcavities

Due to the symmetry, the Maxwell equations could be analytically solved to obtain the properties of modes for regular microcavities. However, there are no strict analytical solutions to the nonregular microcavities, and we are forced to solve the Maxwell equations by the approximated numerical method. The three-dimensional simulation of the microcavity is challenging for even modern computer. Usually, people simplify the three-dimensional Maxwell equation to the two-dimensional Helmholtz equation. For instance, a flat microdisk can be approximate to a two-dimensional case by the effective refractive index method [28] when its height is much smaller than the diameter. For a microsphere, although it is not flat, it can also be reduced to the two-dimensional case because the fundamental modes are confined in the two-dimensional equator plane.

For the two-dimensional Helmholtz equation, the numerical solution is carried out by the popularly used boundary element method (BEM) [29–31] in frequency domain and the finite difference time domain (FDTD) [32,33] method, to achieve the field pattern and the quality factor of the resonances. These methods can be well performed in a personal computer and can solve the microcavity with nkr (n is the refractive index, k is the wave vector, and r is the mean radius of the cavity) as large as few hundred and the quality factor up to 10^{10}. The two-dimensional approximation is proven by various experiments though three-dimensional microcavities are actually used. In general, the two-dimensional model can provide the free-space range and the emission properties of the modes that are well consistent with the experiments but cannot exactly give the mode frequencies and the quality factors.

2.2 Ray dynamics

The wave solution for the nonregular cavity is costly and lack of essential physics. A simpler and more intuitive way to comprehend the behavior of light in the cavity is the ray trajectory (the geometrical size of a microcavity is typically much larger than the wavelength of the interest, i.e., short wavelength limit). Figure 3(a) shows the ray trajectory in

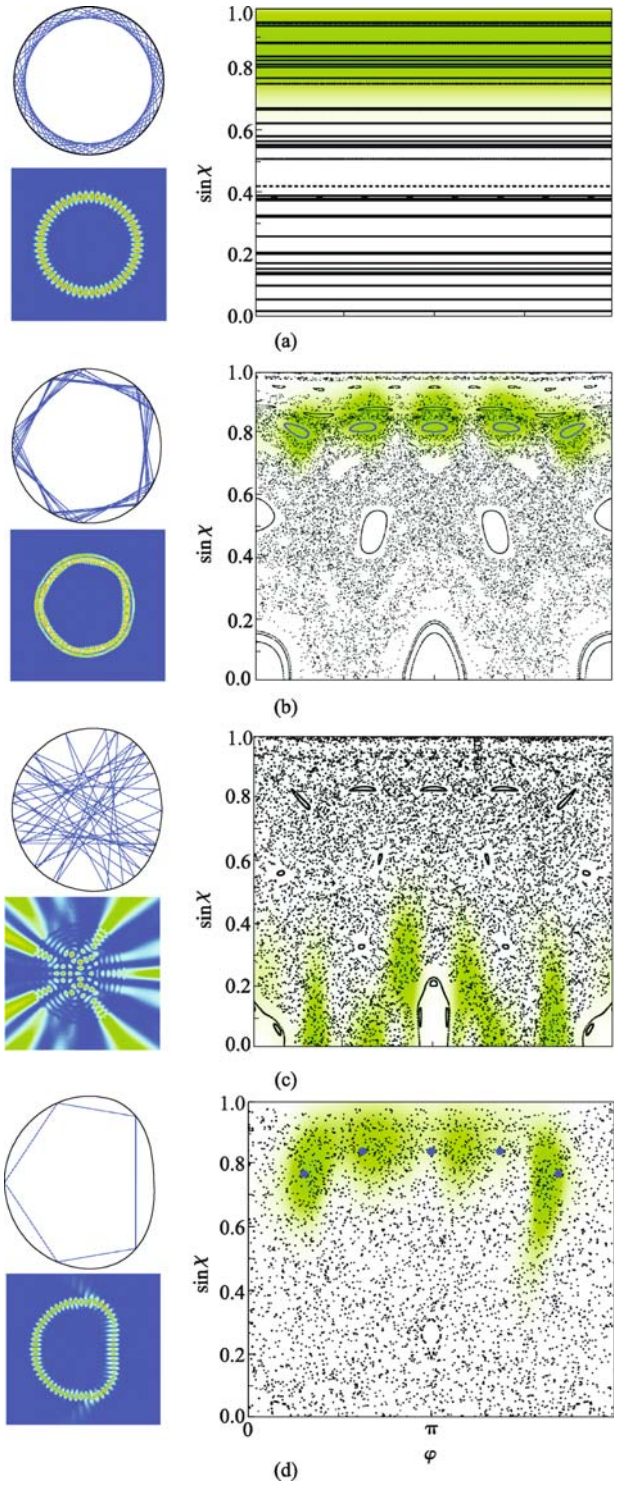

Fig. 3 Ray dynamics, wave field distribution, and Husimi distribution of modes in a hybrid half-quadrupole-half-circular cavity with deformations of (a) 0.00, (b) 0.10, (c) 0.20, and (d) 0.30, respectively (The ray trajectories correspond to the quasi-periodic, stable period-5 orbit, chaotic, and unstable period-5 orbit, respectively. The field patterns are whispering gallery mode, periodic orbit, chaotic mode, and scar mode, corresponding to the ray trajectories, respectively. The Husimi distributions of these modes are plotted in the phase space, respectively)

the circular cavity, where the ray reflects when it hits on the boundary. Due to the rotating symmetry of boundary, the rays should be continuously reflected with the same incidence angle. However, for ARCs, the incidence angle keeps varying when it is reflected on the boundary. As we can see in Fig. 3, the ray trajectories seem no longer regular and even chaos appears. Here, we take the hybrid half-quadrupole-half-circular (HQHC) cavity as an example, which has the boundary described by

$$R(\varphi) = 1 + \frac{\varepsilon[1 + \mathrm{sign}(\cos\varphi)]}{2\cos(2\varphi)}.$$

The ray dynamics in the cavities is very similar to Billiard that has been extensively studied in quantum chaos [34,35]. Ray dynamics is typically studied by introducing the Poincaré surface of section (SOS), where each point in this phase space corresponding to the ray reflection on the boundary by Birkhoff coordinate $[\phi, \sin\chi]$. Here, ϕ is the angular location on the boundary, and χ represents the incidence angle, as shown in Fig. 2(b). Figures 3(a)–3(d) are the SOS of the HQHC cavity with $\varepsilon = 0.0,0.1,0.2,0.3$, respectively. It is obvious that, for $\varepsilon = 0$, i.e., the circular boundary, the SOS consists of lines, corresponding to the unchanged incidence angle with sequence reflections. For nonzero deformation, however, the SOS is the mixed phase space, containing both regular and chaotic motions. There are three different types of ray motion: the Kolmogorov-Arnold-Moser (KAM) curves, the islands, and the chaotic sea, corresponding to quasi-periodicity, periodicity, and chaotic motion of rays, respectively [26]. When the deformation increases, the phase space becomes more chaotic with the KAM curve broken and the stable islands vanished.

It is important to compare the ray dynamics and wave solution in the same platform, and this can be done in the phase space. Because of the wave nature of the light, the wave solution actually contains the uncertain relationship of the position and the incidence angle (in other words, they cannot be determined at the same time). To obtain the phase space presentation of wave function, Husimi presentation works well for it, in which the eigenstate, i.e., mode field distribution, is projected onto a coherent state. In the ray-wave correspondence in microcavities, the projection should be operated with the overlap of the cavity field and the minimum-uncertainty Gaussian beams [36,37]. Figures 3(a), 3(b), and 3(c) present the Husimi distributions of a whispering gallery mode, stable period-5 mode, and chaotic mode in HQHC, respectively. It can be found that the both patterns are consisting with the corresponding SOS patters for the given modes. In addition, there is also another type of mode that do not correspond to regular or chaotic ray motions, as in Fig. 3(d), the wave solution shows that modes have localized on the unstable period orbits, is the so-called scar modes [38].

2.3 Mechanism of directional emission

In this section, we introduce the escape mechanism in the ray dynamics, since our cavity is an open billiard system. When the ray's incidence angle is near or below the critical angle, obviously, partial light will refractively leak out of the cavity. For regular modes (KAM curves and islands), the field distributions, especially the emission directions of the interest, are easy to predict. While for the chaos trajectories, an intuitive picture is that their field distributions have no directional selectivity. To explain the basic concept in the ray dynamics, we here introduce the two kinds of leaking mechanisms out of the cavity:

1) The ray directly refracts out when the incidence angle reaches the critical angle. In this case, the reflection coefficient can be present by the Fresnel's law.

2) The tunneling mechanism. In the curvature surface, the ray has a certain probability to tunnel out even when the ray incidence angle is larger than critical angle. This could be done by modifying to Fresnel's law.

In an ARC, the incident angle is not conserved, so that rays do not uniformly leak out from boundary. Anyway, the escape probabilities by these two ways depend on the distance between the point and the critical line in the SOS. Thus, the emission directionality, which is our focus in this review, is strongly dependent on the structures of SOS. Ten years ago, Nöckel and Stone [26] introduced the invariant curve in the phase space of ray dynamics to explain the directional emission of an ARC. In this model, the rays diffuse along the curve, so the light trend to leak out at the place where the $\sin\chi$ has the minimum values. However, Schwefel et al. [39] point out that the adiabatic theory has been limited to the small deformation case, and they proposed the short time dynamics to predict the directional emission for large deformation ARCs. At large deformation, the rays will quickly leave the invariant curve and leak out. The ray's motion in phase space will be the domain by the geometry of unstable manifold (Fig. 4(a), blue lines). In this case, the directional emission positions are determined by the intersections between the manifold and the critical line, instead of the intersection between the invariant curve and the critical line.

As shown in Fig. 4(a), the unstable manifold of HQHC with $\varepsilon = 0.2$ has a smaller area of intersection, which corresponds to the high directionality, and the directional emission could be directly seen in the near field distribution (Fig. 4(a) inset). In addition, comparing the far field intensity by the Fresnel's law weighted ray dynamics and BEM, the directionality are consisted. In another way, the rays motion near the critical line have all been domain by the unstable manifold near it, and a direct result is that high Q modes will all have the similar directionality because they obey the same motion when they leak out, leading to the so-called university directionality emission. This has been proven in varied cavity shape in both experiment and numerical simulation [40,41].

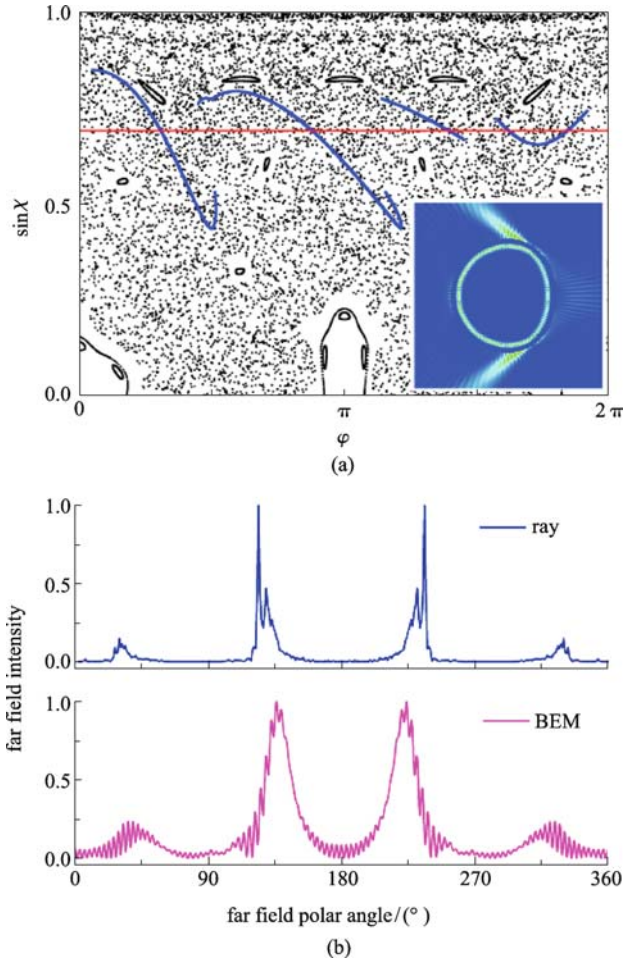

Fig. 4 (a) SOS and unstable manifold of HQHC with deformation of 0.20 (inset: near field pattern of fundamental whispering gallery mode); (b) far field intensity by ray dynamics and wave solution

As we can see in Fig. 5, the quality factor of whispering gallery mode in HQHC decreases with deformation increasing. Due to the whispering gallery, modes in HQHC are localized upon the critical lines as stable or unstable period orbit (Figs. 3(b) and 3(d)), and the modes quality factor are very high even phase space are predominantly chaotic. We could expect that, in a circular like ARC with KAM curve broken near the critical line in phase space, there are always whispering gallery-like modes with the directionality determined by the unstable manifold, which would lead to the high Q and directional emission.

3 Experimental progress in ARCs

After the first demonstration of directional emission in a deformed disk laser [42], both two- or three-dimensional ARCs with different shapes have been proposed and realized since then. For two-dimensional microcavities,

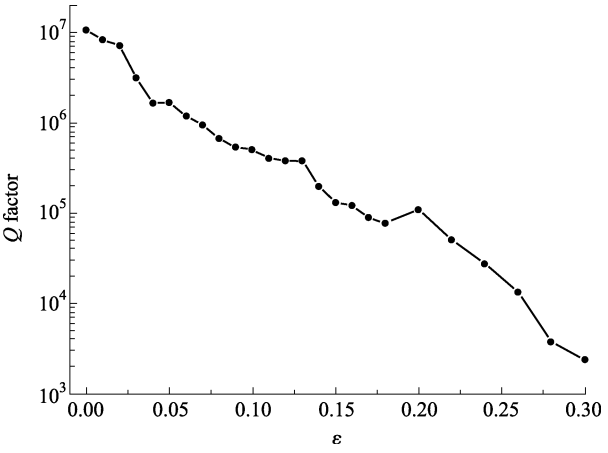

Fig. 5 Quality factor of $TM_{53,1}$ in HQHC evolution with deformation

popular shapes, such as ellipse, quadrupole, stadium, or quasistadium, have been intensively studied. While in the case of three-dimensional ARCs, only a few physical systems are present. In this section, we briefly review the experimental progress in ARCs and focus on the directionality emission and quality factors of their modes, though other aspects are also important for ARC research, such as novel modes and ray dynamics are especially related to quantum and classical chaos. In the following, we first introduce several early experiments in ARCs and then summarize different ARCs according to their boundary shapes.

As mentioned above, the first ARC was reported experimentally by Levi et al. in 1993 [42]. In order to control both the direction and intensity of light output both in the microdisk's plane and in the vertical direction perpendicular to the disk plane (which is also one of the main motivations of studying ARCs until today), they introduced a linear grating around the circumference of the disk or deforming the disk into an appropriately adiabatic egg shape. In this work, they demonstrated that deformed shape did not dramatically degrade quality factors (~150) of the whispering gallery modes (thus did not increase the lasing threshold) [42]. Subsequently, Mekis, Nöckel, Chen, Stone, and Chang investigated the ray chaos and Q spoiling in three-dimensional lasing droplets (formed by a Berglund-Liu vibrating orifice generator that produces a monodispersed stream of ethanol droplets containing Rhodamine-B dye) [43]. The boundary shape of the deformed droplets could be described by the equation

$$r(\theta) = 1 + \varepsilon(\cos^2\theta + 1.5\cos^4\theta),$$

where θ is the polar angle, and ε parameterizes the size of the deformation. The deformed droplets exhibited the highest lasing intensity output centered roughly at $\pm 30°$ from the equator for the prolate sphere. The deformation amplitude of such a droplet is difficult to control. To overcome this difficulty, Moon et al. presented a method of controlling and measuring the deformation amplitude of an ink-doped liquid jet [44]. In their setup, an Ar gas flowed through a glass tube (with end diameter of ~1.5 mm) normal to the liquid jet (2 mm away). As the gas flowed, the lateral aerodynamic force deformed the circular jet to roughly an ellipse. Thus, the deformation of the liquid jet could be highly controlled by the rate of the gas flow. In their experiment, when the deformation ranged from 2.5% to 8.5%, the highly directional lasing was observed under the pump pulse from an Nd:YAG laser. In addition, the effective quality factor decreased with the deformation increasing, i.e., quality factor spoiling effects. For example, the quality factors were 4×10^4, 1.5×10^3, and 7×10^2 when the deformations are 2.5%, 6.5%, and 8.5%, respectively. These three works could be the thought the early experimental investigations of ARCs. Since then, more and more people paid their attention on both theoretical and experimental studies of ARCs, especially after two facts: 1) Nöckel and Stone proposed the solutions of wave equation for ARCs and revealed interesting frequency-dependent effects characteristic of quantum chaos in 1997 [26]. 2) The advance of modern micro/nano fabrication technology.

3.1 Quadrupole-shaped ARCs

The typical (maybe the most popular) ARC is the quadrupole shapes with the boundary equation $r(\theta) \propto 1 + \varepsilon\cos(2\theta)$. The quadrupole shape may be a disk or a crossing section of a cylinder, partly due to the development of modern fabrication technologies. The directional lasing emission (visible) of a quadrupole-type ARC was first observed in a liquid dye column by Nöckel et al. in 1996 [45] and partly explained using ray dynamics in phase space in case of the low-index material cavity.

Two years later, in high-index semiconductor material cavity, Gmachl et al. [46] realized high-power directional quantum-cascade lasing emission (mid-infrared, wavelength of 5.2 μm) from the so-called "flattened" quadruple type ARC (with the boundary $r(\theta) \propto [1 + 2\varepsilon\cos(2\theta)]^{1/2}$), as shown in Fig. 6(a). In this experiment, a power increase in the favorable far-field directions could be obtained up to three orders of magnitude over the conventional circularly symmetric lasers. In the case of small deformation (for example, $\varepsilon = 4\%$), they argued that refractive escape of chaotic whispering gallery orbits (known as invariant curve) still played the central role even for the high-index semiconductor material, similar to the low-index material cavity [45], as shown in Fig. 6(b) (the Husimi distribution is similar to Fig. 6(d)). However, at larger deformations (for example, $\varepsilon = 15\%$), they observed a very different type of laser resonance, i.e., bow-tie modes, which also offered highly directional and high-power emission (Fig. 6(c)). In ray model, these bow-tie modes correspond to the

stable resonance islands in the Hamiltonian quantum dynamics. Similar results were obtained in quadrupole-shaped GaAs-AlGaAs quantum cascade microlasers, which were emitted at long-wavelength (λ = 10 μm) [47].

As just mentioned, the bow-tie modes do not exist in low-index ARCs (such as silica disks or cylindrical dye jets). For these low-index cavities with high deformation, neither stable resonance islands nor stable periodic orbits exist upon the refraction line in the ray-optics model. Thus, directional emission would come from the chaotic whispering gallery modes, which have no real mode structures in the lasing spectrum. Nevertheless, a dense set of unstable periodic orbits still exist in the chaotic sea though they cannot be found in the classical dynamics. There exist extra and unexpected concentrations, i.e., scars of eigenstate density near unstable periodic orbits. In 2002, Lee et al. [49] experimentally observed the scarred modes in asymmetrically deformed microcylinder lasers (liquid jet). This observation is very important since they not only give rise to directional emission but also possess mode-like structures in the emission spectrum. Furthermore, the observed scarred modes have very high quality factors of 3×10^6, two orders of magnitude higher than that expected from the refractive escape of the chaotic whispering gallery modes. The scarred modes are also observed in asymmetrically optically pumped GaN (refraction index $n = 2.65$) microlasers [50] at the lasing wavelength of 375 nm and electrical pumped GaAs/$Ga_{0.51}In_{0.49}P$ ($n = 3.4$) lasers at the lasing wavelength of 950 nm [48]. In the picture of Husimi phase space projection, the scarred modes can be clearly present [48]. As shown in Figs. 6(d)–6(f), for small deformation (< 0.05), the modes are constrained to unbroken KAM curves. As the system is driven to chaos (the deformation is increasing), the KAM curves break, and the mode energy is localized at a stable periodic orbit. With the deformation increasing furthermore, the originally islands disappear and orbits become unstable. The mode is still localized near the orbit, the phenomenon known as wave-function scarring [48]. These scarred states are also present at higher deformations, i.e., larger than 0.12.

The quadrupole-shaped ARCs can also be made of organic materials, besides the aforementioned inorganic materials. In 2004, Polson and Vardeny have fabricated a quadrupole-shaped asymmetric microlaser resonator from a π-conjugated polymer film, which has a low refractive index of 1.8 and emits near 630 nm. The observed quality factor is about 600, which may be resulted from the roughness of the cavity boundary [51]. The relatively high quality factors ($> 3\times10^4$) are also obtained in dye (DCM)-doped polymer (PMMA) ARCs (refractive index $n \approx 1.49$), which are fabricated on top of a spin-on-glass buffer layer coated over a silicon substrate [39].

3.2 Stadium-shaped ARCs

In the past few years, the stadium or quasistadium shape has been extensively studied as a popular model of

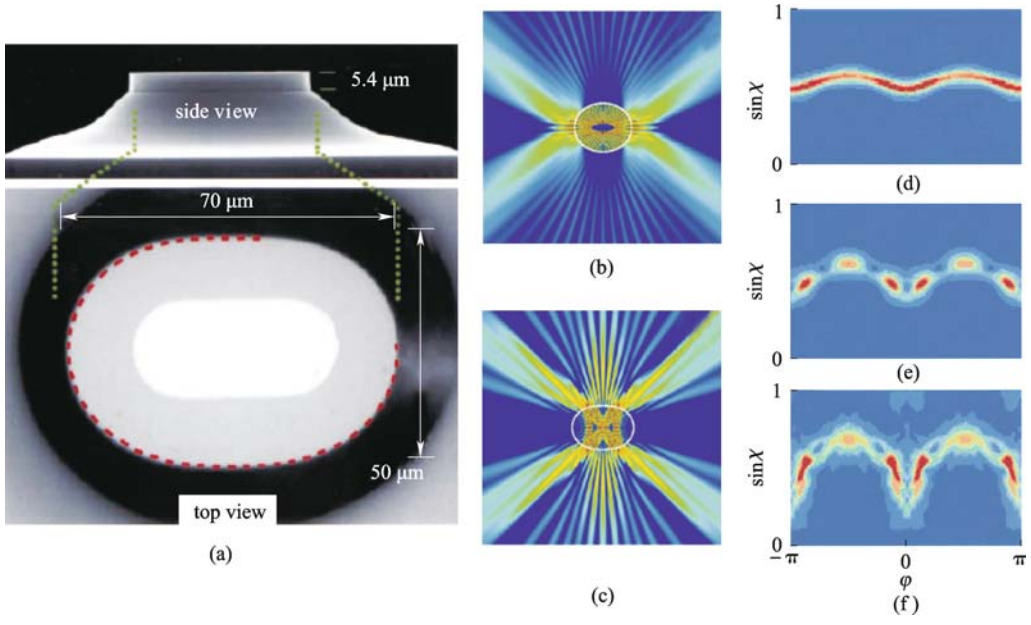

Fig. 6 (a) Side and top view of flattened quadrupolar-shaped cylinder with $\varepsilon = 16\%$ [46]; (b) false-color representation of radiation intensity pattern of chaotic whispering gallery mode for flattened quadrupolar-shaped cylinder with $\varepsilon = 6\%$ [46]; (c) false-color representation of radiation intensity pattern of bow-tie mode with $\varepsilon = 15\%$ [46]; (d) Husimi phase space projections of wave equation solutions for quadrupolar deformed lasers with deformation of 0.03 [48]; (e) Husimi phase space projections of wave equation solutions for quadrupolar deformed lasers with deformation of 0.06 [48]; (f) Husimi phase space projections of wave equation solutions for quadrupolar deformed lasers with deformation of 0.12 [48]

classical and quantum chaos [52–55]. Microcavities with stadium-shaped boundaries (consisting of two half-circles connected by two straight lines) stand for a special kind of ARCs, which are fully chaotic in ray optics picture (no stable ray trajectories, as shown in Fig. 7) though their shapes are very similar to the quadrupole (partially chaotic microcavities). Thus, there is no simply relation between ray trajectories and optical modes. Accordingly, in the presence of the active medium that represents the most important application of microcavity [56–59], it is difficult to predict what type of modes will lase and whether they can be expected to lase stably in fully chaotic cavities. From the viewpoint of fundamental physics, the two-dimensional stadium shape for lasing may be the important application in the research field of nonlinear dynamics.

Recently, it has been pointed out theoretically that in the stadium resonant cavity, laser action can occur on a single spatially chaotic wave function [60]. The stable single-mode lasing state corresponds to a particular metastable resonance of a cavity that wins a competition among multiple modes with positive net linear gain and has a distinct lasing threshold. Shortly, under the help of single-quantum-well GaAs/AlGaAs structure, a quasistadium laser diode has been demonstrated. On one hand, with the increase of the injection current, the intensity of the output light from this microstadium shows a threshold phenomenon. On the other hand, a sharp narrowing of the optical spectrum above the threshold is also observed [61]. By using a nonlinear dynamical model, it has also been theoretically and experimentally reported that the interaction (between two modes belonging to different symmetry classes) can result in the typical nonlinear phenomenon of the locking of two modes, which breaks the symmetry of the lasing pattern in a symmetric stadium resonant cavity [62]. In both quasistadium experiments, high directional emission can be observed, but quality factors are typically low (smaller than one hundreds). Higher quality factors (more than 3000) at near infrared have been obtained in GaAs stadiums, where typically scar modes locate near unstable periodic orbits [63]. When such a mode consists of several unstable period orbits, the interference of partial waves propagating along the constituent orbits may minimize light leakage at certain major-to-minor-axis ratio [64], and this fact has been demonstrated experimentally [63].

Emission directionality is vital because it can be applicable for beam switching and splitting. For this, Choi et al. [65] has fabricated the AlGaAs/GaAs three-quantum-well quasistadium laser diodes with two electrodes and succeeded in controlling directional laser emission by applying different currents to each electrode. The scanning electron microscope image of the device is shown in Fig. 8(a). Figure 8(b) shows the output power versus injection current characteristics that are carried out with continuous wave operation at room temperature. They have found that the ratio of laser emission with two different directions is proportional to the ratio of currents injected into two electrodes. As depicted in Fig. 8(c), the quasistadium laser supports four emission directions A, B, C, and D. To describe the light intensity distribution, they introduce intensity ratios γ_{AB} and γ_{DC}, defined as I_A/I_B, I_D/I_C, respectively. Here I_A, I_B, I_C, and I_D denote the light intensities of four directional beams corresponding to A, B, C, and D, respectively. Figure 8(d) shows the change of γ_{AB} and γ_{DC} as the radio of injection current is increased, while the total current maintains unchanged.

Stadium-shaped microlasers can also be fabricated with organic materials. In general, inorganic semiconductors present the advantages of electrical injection, controlled bur difficult multistep technology; while organic materials behave low-cost and simplicity of the fabrication. In addition, most polymers have a lower refractive index than classical semiconductors, which may lead to different physical behaviors. Lebental et al. [66,67] have reported a stadium-shaped polymer (PMMA) microlaser in which DCM dye is the active guest. The quality factor is demonstrated to be greater than 6000, and the laser emission is highly directional (with the full wave at half maximum (FWHM) of only 15 degree in the far-field pattern). However, in this work, they have not theoretically explained the high-Q modes of polymer microstadium. In 2007, with polymer microstadiums (rhodamine 640 perchlorate dye doped cresol novolac resin), Fang and Cao also observed the lasing action. Their numerical

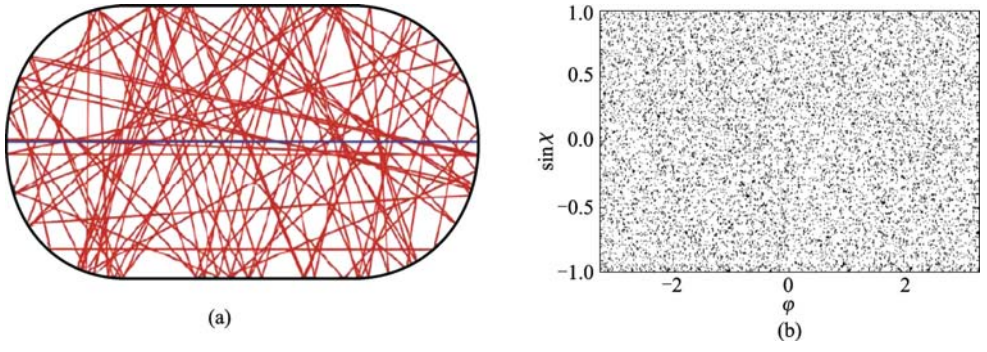

Fig. 7 (a) Ray dynamics of stadium-shaped microcavity; (b) surface of section of stadium-shaped microcavity

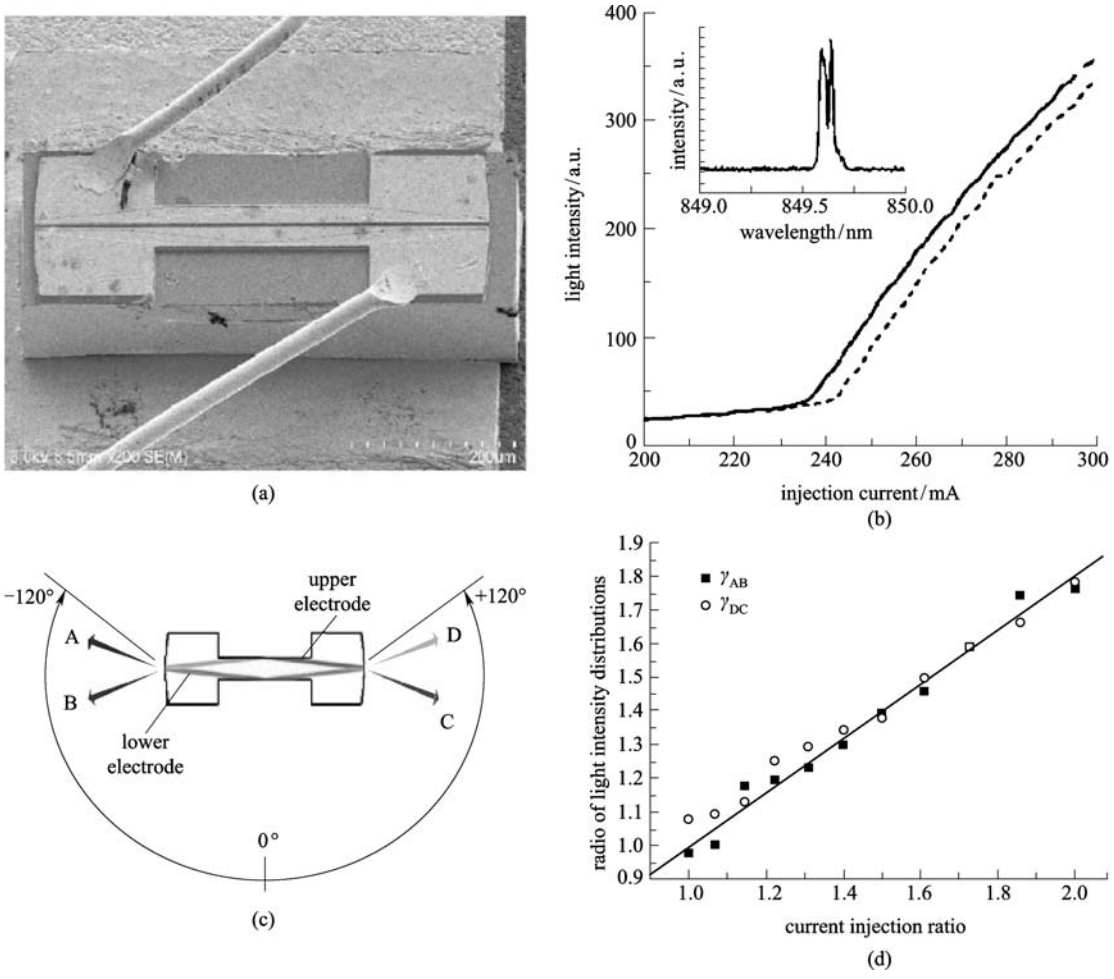

Fig. 8 (a) Scanning electron microscope image of GaAs three-quantum-well quasistadium laser diode with two electrodes; (b) output power versus injection current characteristics for GaAs three-quantum-well quasistadium laser diode; (c) schematic diagram of far-field measurement; (d) curve of injection current ratios to ratios of light intensity distributions (These figures are from Ref. [65])

simulations reveal that the lasing modes are so-called scar modes consisting of multiple unstable period orbits even in the low-index polymer microstadium [68]. Very recently, stadium-shaped microcavity is also used to study divergent Petermann factor of interacting resonances [69].

3.3 Spiral-shaped ARCs

One of the most promising applications of ARCs is the low-threshold microlaser and single-photon source with highly directional emission. However, the above-mentioned ARCs will generate at least two output beams (i.e., multi-direction), which limit their applications, for example, the collection of the output light. Thus, an ARC possessing highly unidirectional emission characteristic is essential. To achieve such a unidirectional emission, Chern et al. [70] has proposed a novel design of ARCs, i.e., the spiral-shaped microcavities, as shown in Fig. 9(a). The boundary of the crossing section of the micropillar is defined by the equation

$$r(\phi) = r_0\left(1 + \frac{\varepsilon}{2\pi}\phi\right),$$

where ε is the deformation parameter, and r_0 represents the radius of the spiral at polar angle $\phi = 0$. The crossing section creates a "notch" when it jumps back to the position at $\phi = 2\pi$. The multiple quantum-well spiral microcavities are optically excited (pulsed) at normal incidence to the top face of the micropillar. At the low pump power, the output light behaves the characteristic of spontaneous emission. With the pump intensity increasing, it produces an obvious lasing action. The pump threshold of 500 kW/cm^2 has been observed, as shown in Fig. 9(b). With the help of an intensified charge couple device (ICCD), a highly unidirectional emission can be demonstrated (Fig. 9(c)). The distribution of a quasinormal mode is also shown in Fig. 9(d).

After the first optically pumped experiment of spiral-shaped ARCs, the current-injection spiral-shaped microcavity disk laser diodes have also been demonstrated [71]. Similarly, the spiral can be fabricated with polymer

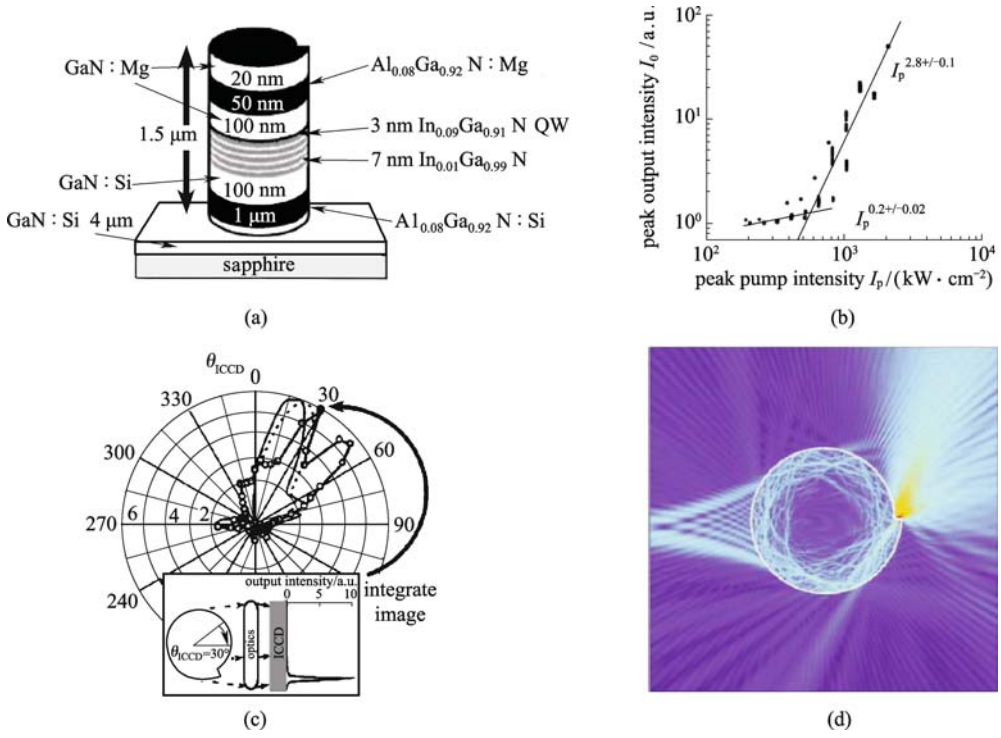

Fig. 9 (a) Structure of InGaN multi-quantum-well spiral-shaped microcavity (QW: quantum well); (b) peak output intensity versus peak pump intensity; (c) unidirectional far-field emission pattern of spiral; (d) real-space false color plot of modulus of electric field for calculated quasibound mode (All these figures are from Ref. [70])

[72,73]. Scarred resonances, which are promising phenomena in quadruple and stadium, quasi-scarred modes have been also investigated in spiral-shaped microcavities [74–76]. Kwon furthermore demonstrate a spiral-shaped dielectric microcavity support not only quasi-scarred resonance modes but also high-Q whispering gallery-like modes [77]. The directionality of whispering gallery-like mode lasing is discussed in Ref. [78]. For more applications, the spiral-shaped microcavity lasers are demonstrated to operate by pumping with continuous-wave current injection [79,80]. Very recently, the modified spiral structures have been reported, such as ring-spiral coupled microcavities [81], waveguide-coupled spiral-shaped microdisk resonators [82].

3.4 Limaçon-shaped ARCs

It should be emphasized here that the spiral-shaped ARCs suffer from large loss (typical quality factors are of the order of one hundred) upon deformation though they support highly unidirectional emission. For potential applications, an essential requirement of ARCs is combining directional light output and ultralow loss (i.e., ultrahigh quality factor). In 2008, Wiersig and Hentschel proposed a deformed microdisk with the limaçon boundary $r(\phi) = r_0(1 + \varepsilon\cos\phi)$ in the polar coordinates, as shown in Fig. 10(a) [83]. In the ray-optic picture, the ray dynamics is predominantly chaotic, but the wave localization on the unstable period orbits (above the refraction line) leads to the formation of high-Q scar modes. The output directionality is universal for all the high-Q scar modes because the corresponding escape routes of rays are similar, as shown in Fig. 10(b). High quality factors (10^6–10^7) have been predicted in this work.

Shortly after the theoretical proposal, several groups have realized this kind of limaçon-shaped microcavities in experiment. In Ref. [84], Yan reported quantum cascade

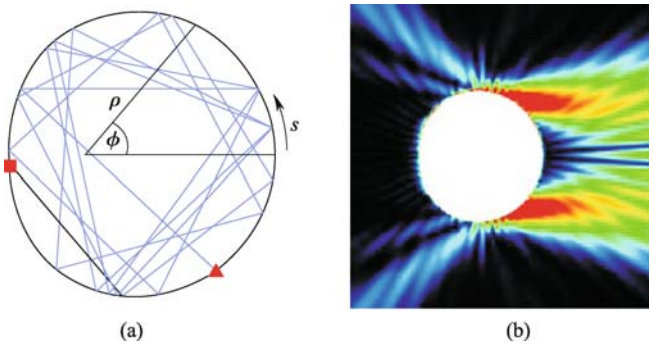

Fig. 10 (a) Chaotic ray trajectory in limaçon cavity with the deformation of 0.43; (b) field distribution of TE mode in limacine, showing highly unidirectional (All these figures are from Ref. [83])

lasers emitting at 10 μm with a limaçon-shaped semiconductor microcavity. Highly directional emission (with far-field divergence angle of 33°) and relatively high quality factor (>1000) have been observed. While in Ref. [85], Yi et al. reported a limaçon-shaped InGaAsP semiconductor microcavity laser in near infrared (around 1593 nm) with the deformation of 0.43. When the laser is continuously pumped with current injection, the lasing far-field divergence angle is around 40°, and the quality factor is higher than 22000. Recently, several groups have also observed the unidirectional emission in different material fabricated limaçon microcavity [86,87].

3.5 Three-dimensional deformed microspheres

The above-mentioned quadrupole, stadium, spiral, and limaçon cavities are known as two-dimensional ARCs and obtain tremendous success but usually exhibit relatively low experimental quality factors (typically smaller than 100000), as well as high pump thresholds for microlasing. Thus, people have strong interest in three-dimensional ARCs since they may provide better confinement of photons in the cavities. The first three-dimensional ARC is deformed droplet microspheres [43,88]. Droplets are very suitable for tunable deforming but suffer from the fast evaporation. For practical applications, solid-state systems are especially desired. To prepare three-dimensional deformed silica microspheres, Lacey et al. [89] fuse two microspheres with similar sizes together by a CO_2 laser beam. The final deformed microspheres have diameters of ~200 μm, and the deformation can be controlled from 1% to 7%. The deformed silica microspheres support not only highly directional emission but also very high quality factors (more than 10^7). The authors declare that the ultrahigh quality factor results from the evanescent escape, not the refractive leakage. To explain the directional emission, the authors think that the escape is dominated by the phase space structures as in the two-dimensional quadrupole, at small deformations [90].

The method preparing such a deformed microsphere is effective but complicated. To fabricate high quality deformed silica microspheres, Xiao et al. [91] successfully developed a simple but effective method in which only one microsphere is necessary. First, individual microspheres with diameters ranging from 30 to 100 μm are generally fabricated by using a CO_2 laser. For such an undeformed microsphere, the quality factor ranges between 10^7 and 10^8, limited by the scattering losses on residual surface inhomogeneities and our laboratory environment. Second, two opposite sides of the single sphere are arbitrarily chosen to be reheated by a short pulse (duration, 20 ms; beam waist, 36 μm) of the CO_2 laser (power, about 5 W) in turn. Next, the microspheres with a small deformation of the equator plane can be routinely produced, as shown in Fig. 11(a). The deformed silica microspheres have been demonstrated high quality factors of 2×10^7 and four

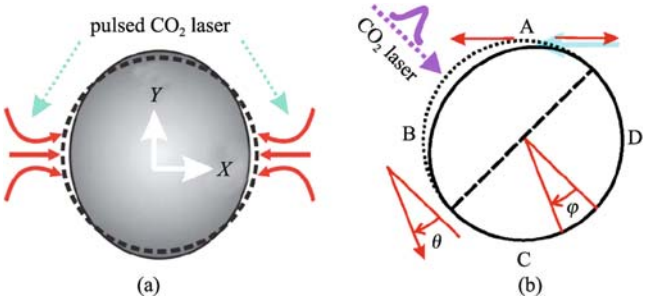

Fig. 11 (a) CO_2 laser pulses (beam waist ~30 μm) reheat microsphere from two opposite sides; (b) CO_2 laser pulses reheat microsphere from one side (The solid curve schematically describes the final shape of the equator plane, while the dotted curve displays a standard circular boundary. These two figures are from Refs. [91] and [92])

obvious emission directions for clockwise or counter-clockwise modes. To reduce the emission directions, the authors optimize their method and only single CO_2 laser pulse is required, as shown in Fig. 11(b) [92]. The boundary of the microsphere equator plane is believed to be deformed to a combination of a half-circle and a half-quadrupole. In this work, the microsphere is covered by Er: Yb phosphate glass, and thus, it allows for studying active deformed microcavity. Different from conventional ARC experiments, the authors adopt direct free-space coupling including the incoupling of the excitation wave and the outcoupling of the resulting microlaser, which are essential for ARCs. The measured threshold is as low as 50 μW. The lasing emission presents high directionality along only two directions centered at 45° and 135°, corresponding to emission points B and A in the deformed side, as shown in Fig. 12(a). From the ray optics (Poincaré surface of section, SOS), the lasing mode is demonstrated the high-Q five-bounce mode (Fig. 12(b)). The expanded SOS has also been illuminated, as the inset of Fig. 12(b). It is obvious that the two center islands have smaller $\sin\chi$ with a difference of more than 0.02, which qualitatively indicates directional emissions there.

The solid-state deformed microspheres have shown some other interesting applications in optics and photonics recently. For example, the directional emission can be used to directly map whispering gallery modes in a deformed microsphere [93]. Deformed microsphere can also be used to study the radiation pressure driven by mechanical oscillation [94] and resolved-sideband cryogenic cooling of an optomechanical resonator [95]. In the presence of single dipole, high-Q deformed microspheres are suitable to investigate cavity QED at low temperature [96].

3.6 Other ARCs

Besides the above-mentioned, many other ARCs with different boundaries have been proposed, for example,

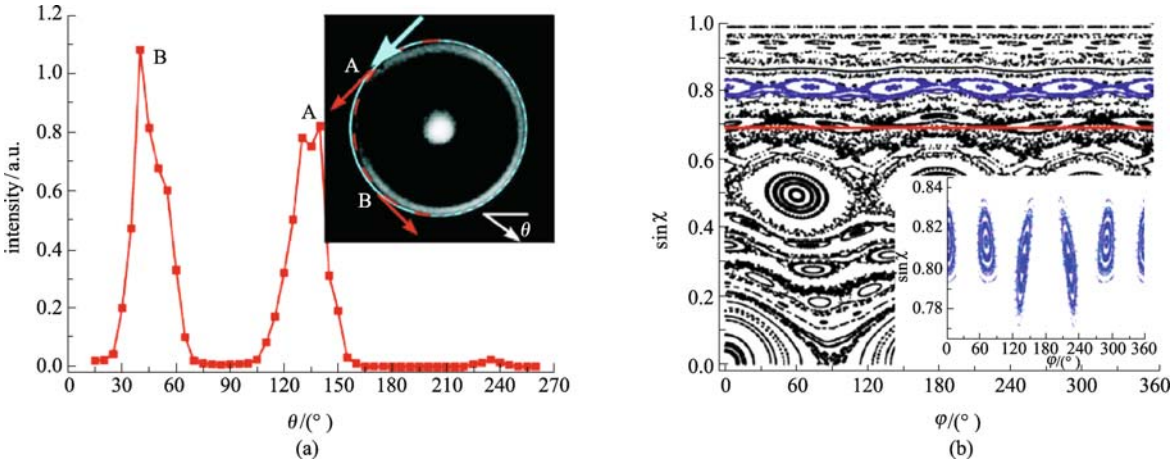

Fig. 12 (a) Far-field emission distribution of lasing at 1552.5 nm in deformed microsphere (The modes are excited in free-space close to point A. Emission spectra are recorded every 5° on the boundary of the microsphere. Inset is the optical image of the equator plane. The solid curve (blue line) draws the boundary of a normal circle, while the dashed curve (red line) describes the boundary of a half-circle and a half-quadrupole with the deformation of 2%); (b) Poincaré SOS (The deformation is 2%. Inset is the expanded SOS of the five-bounce mode) (These two figures are from Ref. [92])

elliptical-shaped microcavities [97,98], hexagon-shaped microcavities [99–102], peanut-shaped microcavity [103], square-shaped microcavities [104–108], and equilateral triangle-shaped microcavities [109,110]. To achieve unidirectional emission, rounded isosceles triangle-shaped microcavity have been suggested, but the quality factors of the round isosceles are only 40 [111]. Even using the interior whispering gallery modes, the quality factors are about 6000 [112]. Another method toward unidirectional emission is introducing a defect in a symmetric cavity [113–118]. However, this approach works only for particular modes, and the existence of nearly degenerate modes with totally different far-field patterns smears out the output directionality.

4 Further work on ARCs

With great progress in both theory and experiment, the study of ARCs has been immerged in various fields, such as microlasing, single-photon source, quantum chaos, ray-wave correspondence, and open quantum system. To our best knowledge, the following points deserve paying more attentions:

1) The applications with both directional collection and directional excitation. Beyond the traditional evanescent near-field coupling, the collimation unidirectional emission of an ARC could be utilized for the efficient output of microcavity laser. An intuitive thought is that the directionality could also allow for the efficient directional excitation, which has been proven recently that 1000-fold enhancement of the pump efficiency in deformed microcylinder compares to circular cross-section microcylinder [119,120].

2) The corrected ray model to comprehend the properties on the ARC. When the size of a microcavity is of the order of several wavelengths, the light lies at the situation between the quantum and classical cases. There are some interesting phenomena in this regime. In the short-wavelength limit, the ray model is valid to study and predict the directional emission characteristics, and a lot of experiments show the ray-wave correspondence in this regime, for example, in case of $nkr > 100$. However, when the cavity size is goes down, the ray optics model is problematic, where the wave nature of light plays an important role. The deviation of ray model has been reported in several cavity shapes, and the corrected ray optics can explain some phenomena [121–124].

3) In the dielectric microcavity, the continuing boundary condition makes the cavity as an opening quantum system, i.e., open billiard, which is used to study quantum chaos. Some interesting physics in this system has attracted more and more attentions, such as chaos assisted tunneling, the dynamics localization, and the scar or quasi-scar mode. On the other hand, the openness of the microcavity can be described by the non-Hermitian Hamiltonian, whose eigenvalues of the system are complex. Some interesting topics include the evolution of the bi-orthogonal quasi-eigenmode dynamics in ARCs, the anticrossing of resonances and the Petermann factor near the exception points [69], the mode trapping, etc.

Acknowledgements The authors acknowledge financial support from the National Natural Science Foundation of China (Grant No. 10821062), the National Basic Research Program of China (Nos. 2006CB921601, 2007CB307001). Zou Chang-Ling, Dong Chun-Hua, and Han Zheng-Fu were supported by the National Fundamental Research Program of China (No. 2006CB921900) and the National Natural Science Foundation of China (Grant Nos. 60537020, 60621064). Xiao Yun-Feng was also supported by the

Research Fund for the Doctoral Program of Higher Education (No. 20090001120004) and the Scientific Research Foundation for the Returned Overseas Chinese Scholars.

References

1. Vahala K J. Optical Microcavities. Singapore: World Scientific, 2004
2. Vahala K J. Optical microcavities. Nature, 2003, 424(6950): 839–846
3. Hood C J, Lynn T W, Doherty A C, Parkins A S, Kimble H J. The atom-cavity microscope: single atoms bound in orbit by single photons. Science, 2000, 287(5457): 1447–1453
4. Gérard J M, Sermage B, Gayral B, Legrand B, Costard E, Thierry-Mieg V. Enhanced spontaneous emission by quantum boxes in a monolithic optical microcavity. Physical Review Letters, 1998, 81 (5): 1110–1113
5. Foresi J S, Villeneuve P R, Ferrera J, Thoen E R, Steinmeyer G, Fan S, Joannopoulos J D, Kimerling L C, Smith H I, Ippen E P. Photonic-bandgap microcavities in optical waveguides. Nature, 1997, 390(6656): 143–145
6. Vučković J, Lončar M, Mabuchi H, Scherer A. Design of photonic crystal microcavities for cavity QED. Physical Review E, 2001, 65 (1): 016608
7. Srinivasan K, Barclay P E, Painter O, Chen J X, Cho A Y, Gmachl C. Experimental demonstration of a high quality factor photonic crystal microcavity. Applied Physics Letters, 2003, 83(10): 1915–1917
8. Ching S C, Lai H M, Young K. Dielectric microspheres as optical cavities: Einstein A and B coefficients and level shift. Journal of the Optical Society of America B, 1987, 4(12): 2004–2009
9. Collot L, Lefevre-Seguin V, Brune M, Raimond J M, Haroche S. Very high-Q whispering-gallery mode resonances observed on fused silica microspheres. Europhysics Letters, 1993, 23(5): 327–334
10. Gayral B, Gerard J M, Lemaitre A, Dupuis C, Manin L, Pelouard J L. High-Q wet-etched GaAs microdisks containing InAs quantum boxes. Applied Physics Letters, 1999, 75(13): 1908–1910
11. Moon H J, Chough Y T, An K. Cylindrical microcavity laser based on the evanescent-wave-coupled gain. Physical Review Letters, 2000, 85(15): 3161–3164
12. Armani D K, Kippenberg T J, Spillane S M, Vahala K J. Ultra-high-Q toroid microcavity on a chip. Nature, 2003, 421(6926): 925–928
13. Maunz P, Puppe T, Schuster I, Syassen N, Pinkse P W H, Rempe G. Cavity cooling of a single atom. Nature, 2004, 428(6978): 50–52
14. McKeever J, Boca A, Boozer A D, Buck J R, Kimble H J. Experimental realization of a one-atom laser in the regime of strong coupling. Nature, 2003, 425(6955): 268–271
15. Noda S, Fujita M, Asano T. Spontaneous-emission control by photonic crystals and nanocavities. Nature Photonics, 2007, 1(8): 449–458
16. Tanabe T, Notomi M, Kuramochi E, Shinya A, Taniyama H. Trapping and delaying photons for one nanosecond in an ultrasmall high-Q photonic-crystal nanocavity. Nature Photonics, 2007, 1(1): 49–52
17. Braginsky V B, Gorodetsky M L, Ilchenko V S. Quality-factor and nonlinear properties of optical whispering-gallery modes. Physics Letters A, 1989, 137(7–8): 393–397
18. Savchenkov A A, Ilchenko V S, Matsko A B, Maleki L. Kilohertz optical resonances in dielectric crystal cavities. Physical Review A, 2004, 70(5): 051804
19. McCall S L, Levi A F J, Slusher R E, Pearton S J, Logan R A. Whispering-gallery mode microdisk lasers. Applied Physics Letters, 1992, 60(3): 289–291
20. Sandoghdar V, Treussart F, Hare J, Lefèvre-Seguin V, Raimond J M, Haroche S. Very low threshold whispering-gallery-mode microsphere laser. Physical Review A, 1996, 54(3): R1777–R1780
21. Aoki T, Dayan B, Wilcut E, Bowen W P, Parkins A S, Kippenberg T J, Vahala K J, Kimble H J. Observation of strong coupling between one atom and a monolithic microresonator. Nature, 2006, 443(7112): 671–674
22. Armani A M, Kulkarni R P, Fraser S E, Flagan R C, Vahala K J. Label-free, single-molecule detection with optical microcavities. Science, 2007, 317(5839): 783–787
23. Gorodetsky M L, Ilchenko V S. High-Q optical whispering-gallery microresonators: precession approach for spherical mode analysis and emission patterns with prism couplers. Optics Communications, 1994, 113(1–3): 133–143
24. Dubreuil N, Knight J C, Leventhal D, Sandoghdar V, Hare J, Lefére-Seguin V, Raimond J M, Haroche S. Mapping whispering-gallery modes in microspheres with a near-field probe. Optics Letters, 1995, 20(14): 1515–1517
25. Cai M, Painter O, Vahala K J. Observation of critical coupling in a fiber taper to silica-microsphere whispering gallery mode system. Physical Review Letters, 2000, 85(1): 74–77
26. Nöckel J U, Stone A D. Ray and wave chaos in asymmetric resonant optical cavities. Nature, 1997, 385(6611): 45–47
27. Narimanov E E, Podolskiy V A. Chaos-assisted tunneling and dynamical localization in dielectric microdisk resonators. IEEE Journal of Selected Topics in Quantum Electronics, 2006, 12(1): 40–51
28. Chin M K, Chu D Y, Ho S T. Estimation of the spontaneous emission factor for microdisk lasers via the approximation of whispering gallery modes. Journal of Applied Physics, 1994, 75 (7): 3302–3307
29. Wiersig J. Boundary element method for resonances in dielectric microcavities. Journal of Optics A: Pure and Applied Optics, 2003, 5(1): 53–60
30. Zou C L, Yang Y, Xiao Y F, Dong C H, Han Z F, Guo G C. Accurately calculating high quality factor of whispering-gallery modes with boundary element method. Journal of the Optical Society of America B, 2009, 26(11): 2050–2053
31. Boriskina S V, Sewell P, Benson T M, Nosich A I. Accurate simulation of two-dimensional optical microcavities with uniquely solvable boundary integral equations and trigonometric Galerkin discretization. Journal of the Optical Society of America A, 2004, 21(3): 393–402
32. Fujita M, Baba T. Proposal and finite-difference time-domain simulation of whispering gallery mode microgear cavity. IEEE

Journal of Quantum Electronics, 2001, 37(10): 1253–1258
33. Guo W H, Li W J, Huang Y Z. Computation of resonant frequencies and quality factors of cavities by FDTD technique and Pade approximation. IEEE Microwave and Wireless Components Letters, 2001, 11(5): 223–225
34. Stöckmann H J. Quantum Chaos: An Introduction. UK: Cambridge University Press, 1999
35. Backer A. Quantum chaos in billiards. Computing in Science and Engineering, 2007, 9(3): 60–64
36. Hentschel M, Schomerus H, Schubert R. Husimi functions at dielectric interfaces: inside-outside duality for optical systems and beyond. Europhysics Letters, 2003, 62(5): 636–642
37. Nöckel J U, Chang R K. 2-D microcavities: theory and experiments. In: van Zee R D, Looney J P, eds. Cavity-Enhanced Spectroscopies. San Diego: Academic Press, 2002
38. Heller E J. Bound-state eigenfunctions of classically chaotic hamiltonian systems: scars of periodic orbits. Physical Review Letters, 1984, 53(16): 1515–1518
39. Schwefel H G L, Rex N B, Tureci H E, Chang R K, Stone A D, Ben-Messaoud T, Zyss J. Dramatic shape sensitivity of directional emission patterns from similarly deformed cylindrical polymer lasers. Journal of the Optical Society of America B, 2004, 21(5): 923–934
40. Schäfer R, Kuhl U, Stöckmann H J. Directed emission from a dielectric microwave billiard with quadrupolar shape. New Journal of Physics, 2006, 8(3): 46
41. Lee S B, Yang J, Moon S, Lee J H, An K, Shim J B, Lee H W, Kim S W. Universal output directionality of single modes in a deformed microcavity. Physical Review A, 2007, 75(1): 011802
42. Levi A F J, Slusher R E, McCall S L, Glass J L, Pearton S J, Logan R A. Directional light coupling from microdisk lasers. Applied Physics Letters, 1993, 62(6): 561–563
43. Mekis A, Nöckel J U, Chen G, Stone A D, Chang R K. Ray chaos and *Q* spoiling in lasing droplets. Physical Review Letters, 1995, 75(14): 2682–2685
44. Moon H J, Ko K H, Noh Y C, Kim G H, Lee J H, Chang J S. Observation of *Q*-spoiling effects on the resonance modes from a noncircularly deformed liquid jet. Optics Letters, 1997, 22(23): 1739–1741
45. Nöckel J U, Stone A D, Chen G, Grossman H L, Chang R K. Directional emission from asymmetric resonant cavities. Optics Letters, 1996, 21(19): 1609–1611
46. Gmachl C, Capasso F, Narimanov E E, Nöckel J U, Stone A D, Faist J, Sivco D L, Cho A Y. High-power directional emission from microlasers with chaotic resonators. Science, 1998, 280 (5369): 1556–1564
47. Gianordoli S, Hvozdara L, Strasser G, Schrenk W, Faist J, Gornik E. Long-wavelength ($\lambda = 10$ μm) quadrupolar-shaped GaAs-AlGaAs microlasers. IEEE Journal of Quantum Electronics, 2000, 36(4): 458–464
48. Gmachl C, Narimanov E E, Capasso F, Baillargeon J N, Cho A Y. Kolmogorov-Arnold-Moser transition and laser action on scar modes in semiconductor diode lasers with deformed resonators. Optics Letters, 2002, 27(10): 824–826
49. Lee S B, Lee J H, Chang J S, Moon H J, Kim S W, An K. Observation of scarred modes in asymmetrically deformed microcylinder lasers. Physical Review Letters, 2002, 88(3): 033903
50. Rex N B, Tureci H E, Schwefel H G L, Chang R K, Stone A D. Fresnel filtering in lasing emission from scarred modes of wave-chaotic optical resonators. Physical Review Letters, 2002, 88(9): 094102
51. Polson R C, Vardeny Z V. Directional emission from asymmetric microlaser resonators of p-conjugated polymers. Applied Physics Letters, 2004, 85(11): 1892–1894
52. McDonald S W, Kaufman A N. Wave chaos in the stadium: statistical properties of short-wave solutions of the Helmholts equation. Physical Review A, 1988, 37(8): 3067–3086
53. Tomsovic S, Heller E J. Semiclassical dynamics of chaotic motion: unexpected long-time accuracy. Physical Review Letters, 1991, 67 (6): 664–667
54. Biham O, Kvale M. Unstable periodic orbits in the stadium billiard. Physical Review A, 1992, 46(10): 6334–6339
55. Heller E J, Tomsovic S. Postmodern quantum mechanics. Physics Today, 1993, 46(7): 38–46
56. Fukushima T, Biellak S A, Sun Y, Siegman A E. Beam propagation behavior in a quasi-stadium laser diode. Optics Express, 1998, 2(2): 21–28
57. Fukushima T. Analysis of resonator eigenmodes in symmetric quasi-stadium laser diodes. Journal of Lightwave Technology, 2000, 18(12): 2208–2216
58. Fukushima T, Harayama T, Davis P, Vaccaro P O, Nishimura T, Aida T. Ring and axis mode lasing in quasi-stadium laser diodes with concentric end mirrors. Optics Letters, 2002, 27(16): 1430–1432
59. Shinohara S, Fukushima T, Harayama T. Light emission patterns from stadium-shaped semiconductor microcavity lasers. Physical Review A, 2008, 77(3): 033807
60. Harayama T, Davis P, Ikeda K S. Stable oscillations of a spatially chaotic wave function in a microstadium laser. Physical Review Letters, 2003, 90(6): 063901
61. Fukushima T, Harayama T. Stadium and quasi-stadium laser diodes. IEEE Journal of Selected Topics in Quantum Electronics, 2004, 10(5): 1039–1050
62. Harayama T, Fukushima T, Sunada S, Ikeda K S. Asymmetric stationary lasing patterns in 2D symmetric microcavities. Physical Review Letters, 2003, 91(7): 073903
63. Fang W, Cao H, Solomon G S. Control of lasing in fully chaotic open microcavities by tailoring the shape factor. Applied Physics Letters, 2007, 90(8): 081108
64. Fang W, Yamilov A, Cao H. Analysis of high-quality modes in open chaotic microcavities. Physical Review A, 2005, 72(2): 023815
65. Choi M, Tanaka T, Fukushima T, Harayama T. Control of directional emission in quasistadium microcavity laser diodes with two electrodes. Applied Physics Letters, 2006, 88(21): 211110
66. Lebental M, Lauret J S, Hierle R, Zyss J. Highly directional stadium-shaped polymer microlasers. Applied Physics Letters, 2006, 88(3): 031108
67. Lebental M, Lauret J S, Zyss J, Schmit C, Bogomolny E. Directional emission of stadium-shaped microlasers. Physical Review A, 2007, 75(3): 033806

68. Fang W, Cao H. Wave interference effect on polymer microstadium laser. Applied Physics Letters, 2007, 91(4): 041108
69. Lee S Y, Ryu J W, Shim J B, Lee S B, Kim S W, An K. Divergent Petermann factor of interacting resonances in a stadium-shaped microcavity. Physical Review A, 2008, 78(1): 015805
70. Chern G D, Tureci H E, Stone A D, Chang R K, Kneissl M, Johnson N M. Unidirectional lasing from InGaN multiple-quantum-well spiral-shaped micropillars. Applied Physics Letters, 2003, 83(9): 1710–1712
71. Kneissl M, Teepe M, Miyashita N, Johnson N M, Chern G D, Chang R K. Current-injection spiral-shaped microcavity disk laser diodes with unidirectional emission. Applied Physics Letters, 2004, 84(14): 2485–2487
72. Ben-Messaoud T, Zyss J. Unidirectional laser emission from polymer-based spiral microdisks. Applied Physics Letters, 2005, 86(24): 241110
73. Tulek A, Vardeny Z V. Unidirectional laser emission from p-conjugated polymer microcavities with broken symmetry. Applied Physics Letters, 2007, 90(16): 161106
74. Lee S Y, Rim S, Ryu J W, Kwon T Y, Choi M, Kim C M. Quasiscarred resonances in a spiral-shaped microcavity. Physical Review Letters, 2004, 93(16): 164102
75. Kim C M, Lee S H, Oh K R, Kim J H. Experimental verification of quasiscarred resonance mode. Applied Physics Letters, 2009, 94 (23): 231120
76. Lee J, Rim S, Cho J, Kim C M. Resonances near the classical separatrix of a weakly deformed circular microcavity. Physical Review Letters, 2008, 101(6): 064101
77. Kwon T Y, Lee S Y, Kurdoglyan M S, Rim S, Kim C M, Park Y J. Lasing modes in a spiral-shaped dielectric microcavity. Optics Letters, 2006, 31(9): 1250–1252
78. Hentschel M, Kwon T Y. Designing and understanding directional emission from spiral microlasers. Optics Letters, 2009, 34(2): 163–165
79. Audet R, Belkin M A, Fan J A, Lee B G, Lin K, Capasso F. Single-mode laser action in quantum cascade lasers with spiral-shaped chaotic resonators. Applied Physics Letters, 2007, 91(13): 131106
80. Kim C M, Cho J, Lee J, Rim S, Lee S H, Oh K R, Kim J H. Continuous wave operation of a spiral-shaped microcavity laser. Applied Physics Letters, 2008, 92(13): 131110
81. Wu X, Li H, Liu L, Xu L. Unidirectional single-frequency lasing from a ring-spiral coupled microcavity laser. Applied Physics Letters, 2008, 93(8): 081105
82. Lee J Y, Luo X, Poon A W. Reciprocal transmissions and asymmetric modal distributions in waveguide-coupled spiral-shaped microdisk resonators. Optics Express, 2007, 15(22): 14650–14666
83. Wiersig J, Hentschel M. Combining directional light output and ultralow loss in deformed microdisks. Physical Review Letters, 2008, 100(3): 033901
84. Yan C, Wang Q J, Diehl L, Hentschel M, Wiersig J, Yu N, Pflugl C, Capasso F, Belkin M A, Edamura T, Yamanishi M, Kan H. Directional emission and universal far-field behavior from semiconductor lasers with limacon-shaped microcavity. Applied Physics Letters, 2009, 94(25): 251101
85. Yi C H, Kim M W, Kim C M. Lasing characteristics of a limacon-shaped microcavity laser. Applied Physics Letters, 2009, 95(14): 141107
86. Song Q, Fang W, Liu B, Ho S T, Solomon G S, Cao H. Chaotic microcavity laser with high quality factor and unidirectional output. Physical Review A, 2009, 80(4): R041807
87. Shinohara S, Hentchel M, Wiersig J, Sasaki T, Harayama T. Ray-wave correspondence in limacon-shaped semiconductor microcavities. Physical Review A, 2009, 80(3): R031801
88. Chang S, Chang R K, Stone A D, Nöckel J U. Observation of emission from chaotic lasing modes in deformed microspheres: displacement by the stable-orbit modes. Journal of the Optical Society of America B, 2000, 17(11): 1828–1834
89. Lacey S, Wang H. Directional emission from whispering-gallery modes in deformed fused-silica microspheres. Optics Letters, 2001, 26(24): 1943–1945
90. Lacey S, Wang H, Foster D H, Nöckel J U. Directional tunneling escape from nearly spherical optical resonators. Physical Review Letters, 2003, 91(3): 033902
91. Xiao Y F, Dong C H, Han Z F, Guo G C, Park Y S. Directional escape from a high-Q deformed microsphere induced by short CO_2 laser pulses. Optics Letters, 2007, 32(6): 644–646
92. Xiao Y F, Dong C H, Zou C L, Han Z F, Yang L, Guo G C. Low-threshold microlaser in a high-Q asymmetrical microcavity. Optics Letters, 2009, 34(4): 509–511
93. Dong C, Xiao Y, Yang Y, Han Z, Guo G, Yang L. Directly mapping whispering gallery modes in a microsphere through modal coupling and directional emission. Chinese Optics Letters, 2008, 6(4): 300–302
94. Park Y S, Wang H. Radiation pressure driven mechanical oscillation in deformed silica microspheres via free space evanescent excitation. Optics Express, 2007, 15(25): 16471–16477
95. Park Y S, Wang H. Resolved-sideband and cryogenic cooling of an optomechanical resonator. Nature Physics, 2009, 5(7): 489–493
96. Park Y S, Cook A K, Wang H. Cavity QED with defect centers and silica resonators. Nano Letters, 2006, 6(9): 2075–2079
97. Zhang L M, Wang Y X, Zhang F J, Claus R O. Observation of whispering-gallery and directional resonant laser emission in ellipsoidal microcavities. Journal of the Optical Society of America B, 2006, 23(9): 1793–1800
98. Whittaker D M, Guimaraes P S S, Sanvitto D, Vinck H, Lam S, Daraei A, Timpson J A, Fox A M, Skolnick M S, Ho Y L D, Rarity J G, Hopkinson M, Tahraoui A. High Q modes in elliptical microcavity pillars. Applied Physics Letters, 2007, 90(16): 161105
99. Yang Y, Xiao Y F, Dong C H, Cui J M, Han Z F, Li G D, Guo G C. Fiber-taper-coupled zeolite cylindrical microcavity with hexagonal cross section. Applied Optics, 2007, 46(31): 7590–7593
100. Braun I, Ihlein G, Laeri F, Nöckel J U, Schulz-Ekloff G, Schuth F, Vietze U, Weiss O, Wohrle D. Hexagonal microlasers based on organic dyes in nanoporous crystals. Applied Physics B, 2000, 70 (3): 335–343
101. Monat C, Seassal C, Letartre X, Regreny P, Gendry M, Romeo P R, Viktorovitch P, Vassord'Yerville M L, Cassagne D, Albert J P, Jalaguier E, Pocas S, Aspar B. Two-dimensional hexagonal-shaped microcavities formed in a two-dimensional photonic crystal on an InP membrane. Journal of Applied Physics, 2003, 93(1): 23–31
102. Wiersig J. Hexagonal dielectric resonators and microcrystal lasers.

Physical Review A, 2003, 67(2): 023807
103. Shang L, Liu L, Xu L. Highly collimated laser emission from a peanut-shaped microcavity. Applied Physics Letters, 2008, 92(7): 071111
104. Poon A W, Courvoisier F, Chang R K. Multimode resonances in square-shaped optical microcavities. Optics Letters, 2001, 26(9): 632–634
105. Ling T, Liu L, Song Q, Xu L, Wang W. Intense directional lasing from a deformed square-shaped organic-inorganic hybrid glass microring cavity. Optics Letters, 2003, 28(19): 1784–1786
106. Lee H T, Poon A W. Fano resonances in prism-coupled square micropillars. Optics Letters, 2004, 29(1): 5–7
107. Wu J H, Liu A Q. Exact solution of resonant modes in a rectangular resonator. Optics Letters, 2006, 31(11): 1720–1722
108. Huang Y Z, Chen Q, Guo W H, Yu L J. Experimental observation of resonant modes in GaInAsP microsquare resonators. IEEE Photonics Technology Letters, 2005, 17(12): 2589–2591
109. Huang Y Z, Guo W H, Wang Q M. Influence of output waveguide on mode quality factor in semiconductor microlasers with an equilateral triangle resonator. Applied Physics Letters, 2000, 77 (22): 3511–3513
110. Wysin G M. Electromagnetic modes in dielectric equilateral triangle resonators. Journal of the Optical Society of America B, 2006, 23(8): 1586–1599
111. Kurdoglyan M S, Lee S Y, Rim S, Kim C M. Unidirectional lasing from a microcavity with a rounded isosceles triangle shape. Optics Letters, 2004, 29(23): 2758–2760
112. Baryshnikov Y, Heider P, Parz W, Zharnitsky V. Whispering gallery modes inside asymmetric resonant cavities. Physical Review Letters, 2004, 93(13): 133902
113. Apalkov V M, Raikh M E. Directional emission from a microdisk resonator with a linear defect. Physical Review B, 2004, 70(19): 195317
114. Fang W, Cao H, Podolskiy V A, Narimanov E E. Dynamical localization in microdisk lasers. Optics Express, 2005, 13(15): 5641–5652
115. Boriskina S V, Benson T M, Sewell P, Nosich A I. *Q* Factor and emission pattern control of the WG modes in notched microdisk resonators. IEEE Journal of Selected Topics in Quantum Electronics, 2006, 12(1): 52–58
116. Wiersig J, Hentschel M. Unidirectional light emission from high-*Q* modes in optical microcavities. Physical Review A, 2006, 73(3): R031802
117. Dettmann C P, Morozov G V, Sieber M, Waalkens H. Directional emission from an optical microdisk resonator with a point scatterer. Europhysics Letters, 2008, 82(3): 34002
118. Djellali N, Gozhyk I, Owens D, Lozenko S, Lebental M, Lautru J, Ulysse C, Kippelen B, Zyss J. Controlling the directional emission of holey organic microlasers. Applied Physics Letters, 2009, 95 (10): 101108
119. Lee S B, Yang J, Moon S, Lee J H, An K, Shim J B, Lee H W, Kim S W. Chaos-assisted nonresonant optical pumping of quadrupole-deformed microlasers. Applied Physics Letters, 2007, 90(4): 041106
120. Yang J, Lee S B, Moon S, Lee S Y, Shim J B, Kim S W, Lee J H, An K. Free-space resonant coupling in a highly deformed microcavity. In: Proceedings of the 11th International Conference on Transparent Optical Networks (ICTON). 2009, Tu.P.17
121. Tureci H E, Stone A D. Deviation from Snell's law for beams transmitted near the critical angle: application to microcavity lasers. Optics Letters, 2002, 27(1): 7–9
122. Rex N B, Tureci H E, Schwefel H G L, Chang R K, Stone A D. Fresnel filtering in lasing emission from scarred modes of wave-chaotic optical resonators. Physical Review Letters, 2002, 88(9): 094102
123. Schomerus H, Hentschel M. Correcting ray optics at curved dielectric microresonator interfaces: phase-space. Physical Review Letters, 2006, 96(24): 243903
124. Altmann E G, Magno G D, Hentschel M. Non-Hamiltonian dynamics in optical microcavities resulting from wave-inspired corrections to geometric optics. Europhysics Letters, 2008, 84(1): 10008